PHYSICAL REVIEW B **96**, 180506(R) (2017)

Coupling of structure to magnetic and superconducting orders in quasi-one-dimensional $K_2Cr_3As_3$

K. M. Taddei,[1,*] Q. Zheng,[2] A. S. Sefat,[2] and C. de la Cruz[1]

[1]*Quantum Condensed Matter Division, Oak Ridge National Laboratory, Oak Ridge, Tennessee 37831, USA*

[2]*Materials Science and Technology Division, Oak Ridge National Laboratory, Oak Ridge, Tennessee 37831, USA*

(Received 14 July 2017; revised manuscript received 27 September 2017; published 20 November 2017)

Quasi-one-dimensional $A_2Cr_3As_3$ (with A = K, Cs, Rb) is an intriguing new family of superconductors which exhibit many similar features to the cuprate and iron-based unconventional superconductor families. Yet, in contrast to these systems, no charge or magnetic ordering has been observed which could provide the electronic correlations presumed necessary for an unconventional superconducting pairing mechanism—an absence which defies predictions of first-principles models. We report the results of neutron scattering experiments on polycrystalline $K_2Cr_3As_3$ ($T_c \sim 7$ K) which probed the low-temperature dynamics near T_c. Neutron diffraction data evidence a subtle response of the nuclear lattice to the onset of superconductivity while inelastic scattering reveals a highly dispersive column of intensity at the commensurate wave vector $q = (00\frac{1}{2})$ which loses intensity beneath T_c—indicative of short-range magnetic fluctuations. Using linear spin-wave theory, we model the observed scattering and suggest a possible structure to the short-range magnetic order. These observations suggest that $K_2Cr_3As_3$ is in close proximity to a magnetic instability and that the incipient magnetic order both couples strongly to the lattice and competes with superconductivity, in direct analogy with the iron-based superconductors.

DOI: 10.1103/PhysRevB.96.180506

Understanding how superconductivity arises from myriad competing ground states and exotic phenomena such as quantum criticality has been an overarching theme in the study of unconventional superconductors, particularly in the well-studied quasi-two-dimensional (Q2D) cuprate and iron-based (FBS) families [1]. Recently, a new family of superconducting quasi-one-dimensional (Q1D) $A_2Cr_3As_3$ (233) materials (with A = K, Cs, Rb) have proven fertile grounds for applying this general narrative to another system which has further lowered dimensionality [2,3].

The 233 family orders in noncentrosymmetric hexagonal $P\bar{6}m2$ space group symmetry with a structural motif of double-walled subnanotubes (DWSs) coaxial to the c axis and of $[(Cr_3As_3)^{-2}]_\infty$ stoichiometry [see Figs. 1(e) and 1(f)] with the A-site ion acting as a spacer/charge reservoir "layer" [2,4,5]. Density functional theory (DFT) calculations predict a Fermi surface built of complex mixtures of the Cr 3d shells with strong Q1D character [3,6,7]. Consequently, predictions of Tomonaga-Luttinger liquid (TLL)/general non-Fermi-liquid physics, Peierls distortions, ferromagnetic (FM) fluctuations/magnetic ordering, and spin-triplet superconductivity have arisen, creating a sea of possible ground states and interactions out of which superconductivity stabilizes [3,5,7–10].

Experimentally, a similarly complex picture has emerged. Non-Fermi-liquid behaviors are observed in transport, nuclear magnetic resonance (NMR). and muon spectroscopy (μSR) measurements, which indicate significant electron correlations and strong magnetic fluctuations [11–13]. More exotically, measurements of the penetration depth find nodes in the superconducting gap while those of the upper critical field find it to be highly anisotropic, greatly exceeding the Pauli-pair-breaking limit, exhibiting an in-plane angular dependence, and even a possible Fulde-Feerel-Larkin-Ovchinnikov state [14–16]. Furthermore, recent angle-resolved photoemission spectroscopy reports find linear behavior of the spectral intensity near the Fermi surface (FS), indicating possible Tomonaga-Luttinger liquid-type physics [17]. Yet these findings have found divergent explanations ranging from unconventional superconductivity with spin-triplet or singlet pairing to conventional phonon-driven scenarios [14,18,19]. This ambiguity arises partially from a lack of direct measurements determining the relevant low-temperature orders. Here, we investigate the structure and magnetic behavior of $K_2Cr_3As_3$ at low temperatures using neutron scattering techniques.

The synthesis of polycrystalline $K_2Cr_3As_3$ was adopted from Refs. [4,11] [as detailed in the Supplemental Material (SM) [20]]. Neutron powder diffraction (NPD) data were collected using the HB-2A powder diffractometer at the High Flux Isotope Reactor (HFIR) of Oak Ridge National Laboratory (ORNL) using wavelengths (λ) of 1.54 and 2.41 Å. High-resolution synchrotron x-ray data were collected at beamline 11BM-B of the Advanced Photon Source (APS) at Argonne National Laboratory (ANL) with $\lambda = 0.414$ Å. Detailed structural analyses were performed using the Rietveld method as implemented in the FULLPROF, GSAS, and EXPGUI software suites [21–24]. Inelastic neutron scattering experiments were carried out on HFIR's triple-axis spectrometer HB-3. Tight collimation was used with a fixed analyzer energy of 14.7 meV.

Our analysis of both the high-resolution x-ray diffraction (XRD) and NPD patterns found models of $K_2Cr_3As_3$ exhibiting the hexagonal space group symmetry $P\bar{6}m2$ to produce the highest-quality fits in accord with previous reports (see SM for details [20]). Considering our room-temperature refinements, the crystallographic data agree with those reported in Ref. [11].

Upon decreasing temperature from 300 to 0.5 K, a, c, and V monotonically contract (Fig. 1). For temperatures $T > 40$ K, a linear thermal expansion is observed (with nearly negligible change for $T < 40$ K) with no evidence of a structural response which might arise from nuclear or magnetic orderings, in

*Corresponding author: taddeikm@ornl.gov

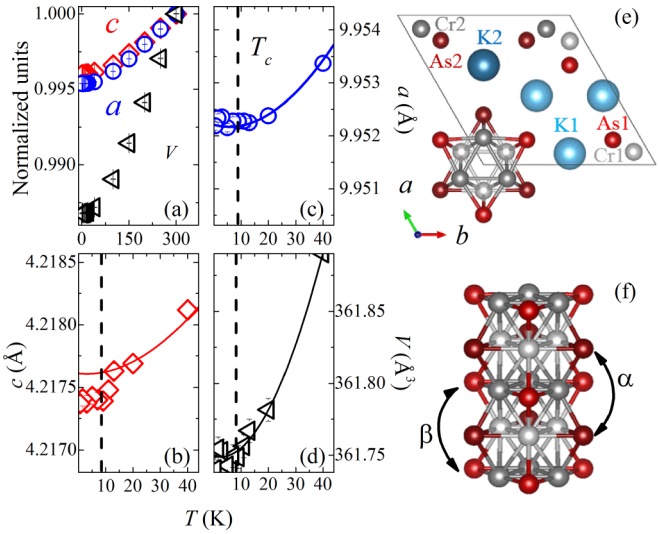

FIG. 1. (a) Temperature dependence of $K_2Cr_3As_3$ lattice parameters a, c, and unit cell volume V extracted from Rietveld refinements of the NPD patterns normalized to 300 K values. (b)–(d) Low-temperature behavior of a, c, and V. Polynomial fits to the high-temperature data (20 K $< T <$ 300 K) are plotted as guides to the eye. All y-axis ranges show the same relative percent change of the parameters. (e) The crystal structure of $K_2Cr_3As_3$ seen along the c axis and (f) the structure of the DWS with angles As2-Cr2-As2 and As1-Cr1-As1 denoted by α and β, respectively. In (a)–(d), the error bars are smaller than the individual data point markers.

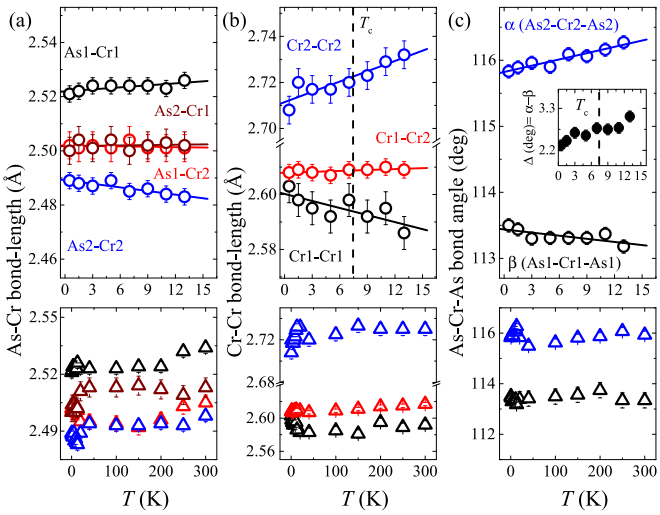

FIG. 2. Temperature dependence of $K_2Cr_3As_3$. (a) As-Cr, (b) Cr-Cr, and (c) As-Cr-As bond lengths and angles as determined from Rietveld refinements. The upper panels focus on $T < 20$ K while the lower panels show all measured temperatures. The inset of (d) shows the degree of noncentrosymmetry as measured by the difference of the two As-Cr-As angles. All scales have been configured to cover similar ranges in percent change of the plotted parameter. Linear fits are provided as guides to the eye.

contrast to DFT calculations' predictions but in accord with featureless transport data [6,7,11]. While it is possible that the relatively large steps in temperature between 300 and 20 K might miss a subtle lattice response, such as that commonly reported for the FBS, comparisons of the high-temperature and low-temperature patterns do not reveal the presence of new peaks, peak splitting, or other evidence of a phase transition (see SM [20]) [25–27].

Such structural stability, despite a predicted Peierls instability, has also been observed in the Q1D chevrel family ($Tl_2Mo_6Se_6$) which shares the DWS structural motif [28,29]. In these materials, the DWS sublattice was found to be rigid due to the significant metal-metal bonding and unique geometry of the DWS. By analogy, we suggest the significant inter- and intra-Cr triangle bonding confounds the expected Peierls distortion which cannot easily lower simultaneously the energies of the inter- and intratriangle bonds [7,29].

Considering the lattice parameters in the range of linear thermal expansion, the coefficient of thermal expansion can be obtained via the expression $\alpha = 1/V_0(V_0 - V)/(T_0 - T)$ (where V can be a or c) which finds α for a, c, and V as 1.9×10^{-5}, 1.7×10^{-5}, and 5.5×10^{-5} K^{-1}, respectively. The expansion along the a axis is slightly larger than along c, as might be expected from the highly anisotropic quasi-1D nuclear structure. This is in accord with reports on $Rb_2Cr_3As_3$ and $Cs_2Cr_3As_3$ as well as pressure studies, both of which found the a axis more sensitive to external and chemical pressure [4,5,30,31]. These values of α are similar to the relatively high values reported for paramagnetic (PM) states of the 11 and various 122 members of the FBS family where strong spin fluctuations are thought to contribute to the thermal expansion [32–39]. As we will show, similar spin fluctuations exist in $K_2Cr_3As_3$ and may be responsible for the large α values.

While no clear signature of a structural phase transition exists, close inspection of the low-temperature behavior (0.5 K $\leqslant T \leqslant$ 20 K) of the c axis reveals a response of the lattice near $T_c \sim 7$ K [Fig. 1(b)]. In this range, the c axis exhibits a contraction just before T_c upon cooling while the a axis remains constant. V undergoes a commensurate contraction reflecting the reduced c axis [Figs. 1(b)–1(d)]. The effect is anisotropic, being observed only in the ostensibly stiffer c axis and appears to correspond to the incipient superconducting transition.

Next, we consider the bonding parameters of the DWS and their behavior across T_c. In general, for 20 K $\leqslant T \leqslant$ 300 K, the DWS geometry exhibits little temperature dependence as the As1-Cr1(2) and Cr1-Cr1(2) bond lengths change by ~0.3% while the As2-Cr1(2) and Cr2-Cr2 bond lengths do not change within the sensitivity of our measurements [Figs. 2(a) and 2(b)]. The relatively minor ~0.4% expansion seen in this temperature range along the c axis is accounted for by the interplaquette spacing while the thermal expansion along the a axis affects the inter-DWS spacing (via As-K bond lengths). The significant metal-pnictide bond-length rigidity seen here is similar to that reported for FBS [Fig. 2(a)] [25,27,40]. This is likely due to the strong antibonding character of these bonds as determined in Ref. [7].

Below 20 K a shift in the DWS bonding behavior is observed. As shown in Fig. 2(b), the previously stoic Cr-Cr bond lengths begin to exhibit temperature dependence. The Cr1(2)-Cr1(2) bonds dilate (contract) by 0.7% (0.9%) as the material is cooled from 13 to 0.5 K, a change larger than twice that from 300 to 20 K. A corresponding contraction

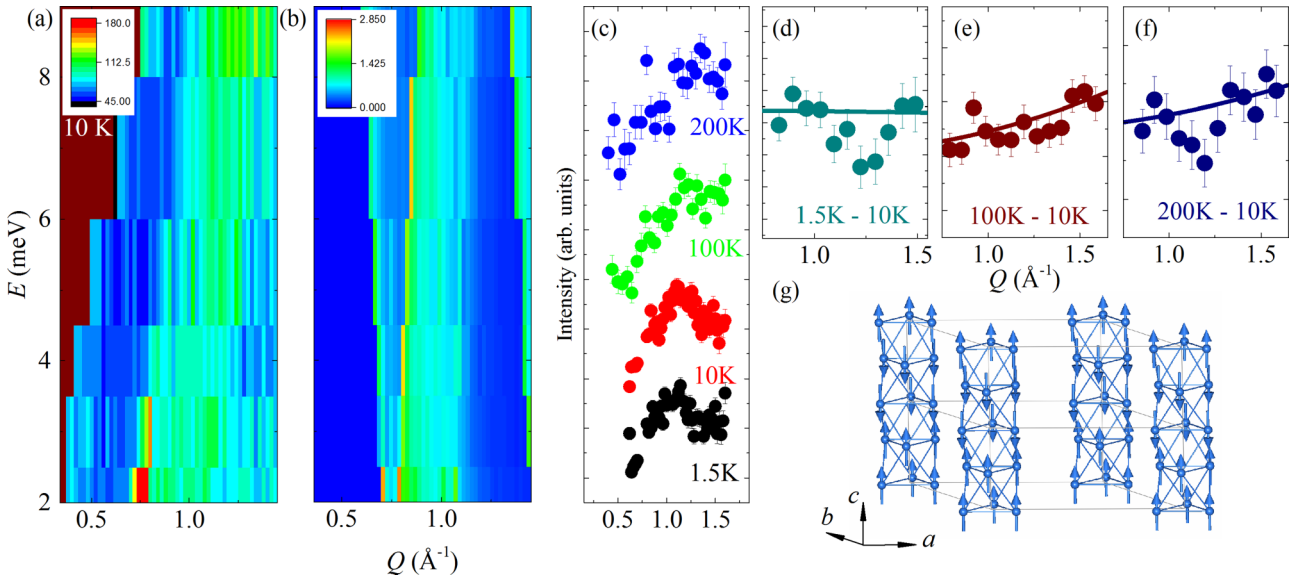

FIG. 3. (a) Neutron spectra intensity map of the dynamic structure factor with the intensity normalized to the monitor. (b) Simulated spin-wave dispersions of the UUDD magnetic structure with arbitrary intensity scale. (c) Q dependence of the scattering intensity for E summed over 2–9 meV for all measured temperatures. Each temperature is offset by an arbitrary y value for visual clarity. Difference curves for the 10 K summed intensity subtracted from the (d) 1.5, (e) 100, and (f) 200 K summed intensities. Lines are added to the plots as guides to the eye. (e) UUDD magnetic structure consistent with $Q \sim 0.75$ Å^{-1} (magnetic space group P_c3c1).

(dilation) of 0.2% (0.24%) is seen in the As1(2)-Cr1(2) bonds. This describes an adjustment of the intra-CrAs plaquette bonding where the larger Cr2 triangle contracts and the Cr1 triangle dilates while the surrounding As matrix remains rigid [as evidenced by the changing As1(2)-Cr1(2) bond lengths] and the inter-DWS spacing remains unchanged [Figs. 2(a) and 2(b)]. The previously discussed c-axis contraction causes a decrease in the interplaquette spacing due to the Cr sites' Wyckoff positions' fixed z components.

The cumulative effect is a decrease in the noncentrosymmetry of the DWS tubes, which can be quantified (as suggested in Ref. [31]) as $\Delta = \alpha - \beta$ [where α and β denote the As2-Cr2-As2 and As1-Cr1-As1 bond angles, respectively; see Fig. 1(f)]. Upon decreasing temperature, α closes and β widens, leading the parameter Δ to decrease from 3 at 13 K to 2.3 at 0.5 K [Fig. 2(c)]. This is somewhat unexpected in light of pressure effect studies that indicated a positive correlation between T_c and Δ [31]. However, we argue that this decrease is a secondary effect due to the competition between superconductivity and short-range magnetic order rather than a direct structural effect of superconductivity.

To probe for incipient magnetic order, inelastic neutron scattering experiments were performed, focusing on low momentum and energy transfers. Figure 3(a) shows a neutron spectra intensity map of the dynamic structure factor $S(Q,E)$ collected at 10 K. A broad column of scattering from 0.75 Å$^{-1} \leqslant Q \leqslant 1.20$ Å^{-1} is clearly seen. The low Q and E values of this feature indicate that it is not likely due to phonons which exhibit a Q^2 in $S(Q,E)$ and have a calculated cutoff in $K_2Cr_3As_3$ of ~4 meV [18,41]. E integrated plots [Fig. 3(c)] for data collected at 1.5, 10, 100, and 200 K show a T-dependent peaklike feature at ~1.2 Å^{-1} visible for $T < 200$ K. Figures 3(d)–3(f) show subtractions of the E-summed data from 10 K. For 100–10 K [Fig. 3(e)], no appreciable change in intensity near ~1.2 Å^{-1} is observed, with the contribution to the difference curve coming only from the increased phonon background at 100 K which exhibits the characteristic Q^2 dependence. On the other hand, 200–10 K [Fig. 3(d)] exhibits a dip in the intensity at $Q \sim 1.2$ Å^{-1}, indicating that the column of scattering is either not present or has a reduced intensity by 200 K. Similarly, 10–1.5 K [Fig. 3(b)] also reveals an intensity difference centered near 1.2 Å^{-1}. The inelastic signal is suppressed not only at high temperatures but also below T_c—significantly this is consistent with both the results of local probes of the dynamic magnetism in $K_2Cr_3As_3$ [nuclear quadrupole resonance (NQR) and Knight shift (KS)] which have suggested short-range magnetic order [12,42,43]. Furthermore, the column closely resembles similar measurements of incipient magnetic order reported for the FBS FeSe and LiFeAs [12,42–45].

The Q onset of the column ~0.75 Å^{-1} [see Fig. 3(a)] is commensurate with a q vector $q_m = (00\frac{1}{2})$ which indexes the feature with hkl of $00\frac{1}{2}$ in the nuclear structure. Using a representational analysis (as implemented in the ISODISTORT software [46]), magnetic structures consistent with $q_m = (00\frac{1}{2})$ were explored, one of which is shown in Fig. 3(g). This model is similar to the "up-up-down-down" (UUDD) magnetic structure predicted in the DFT work of Wu et al. [6]. The UUDD has Cr moments collinear with the crystallographic c axis and exhibits FM correlations within each plaquette, with FM coupling to the neighboring plaquette in one direction along the chain and antiferromagnetic (AFM) along the other [Fig. 3(g)].

To test the various magnetic structures consistent with q_m, Monte Carlo simulations were performed using linear spin-wave theory (as implemented in SPINW [47]) to model the observed inelastic scattering as spin-wave dispersions using the exchange interactions (J) predicted in Ref. [48]. The

simulated inelastic powder spectrum of the UUDD magnetic structure reproduces the general features of our experimental spectrum [Fig. 3(b)] (for more details, see SM [20]). The relatively small region of $S(Q,E)$ covered in our experiment does not allow for a unique determination of the incipient order or for a rigorous determination of the exchange interactions. In this model, the scattering originates from two acoustic spin-wave modes arising from reflections newly allowed by the UUDD structure: hkl of $00\frac{1}{2}$ and $10\frac{1}{2}$. We note that the general scale of the dispersions appears consistent with the predicted J values which put intra-DWS exchanges on the order of $\sim$10 meV and inter-DWS J at >1 meV (see SM [20]). As the latter of these is increased, the branches originating from hkl $00\frac{1}{2}$ and $10\frac{1}{2}$ become distinct and inconsistent with the measurement, suggesting a weak but nonzero inter-DWS coupling.

The authors note that the observed suppression of spin fluctuations below T_c provides a possible explanation for the change in the DWS geometry at T_c. In the metallic FBS, magnetoelastic coupling is strong and spin fluctuations are argued to drive the structural phase behavior affecting subtle bond changes and even structural transitions [49–52]. We speculate that a similar scenario is possible in the metallic $K_2Cr_3As_3$ where changes to the Cr-Cr bonding below T_c may be driven by the reduction of magnetic fluctuations on the Cr sites. In the model shown in Fig 3(g), the reduction of short-range FM correlations within each plaquette could relax the Cr-Cr bonds [Fig. 2(b)]. Similarly, the slight reduction of the c axis near T_c could result from weakened AFM next-nearest plaquette couplings. Irrespective of the magnetic model, predictions of a larger magnetic moment on the Cr2 site anticipate its stronger response to reduced spin fluctuations in the presence of magnetoelastic coupling which is consistent with our results [Fig. 2(b)] [6]. Generally, such an interpretation agrees remarkably well with recent Raman scattering experiments, which report the sudden softening and hardening of Cr modes at $T < 100$ K prospectively due to strong magnetoelastic coupling [53]. Together with our results, this suggests the possible importance of incipient magnetic order to the dynamics of this material and informs the need for further study of its short-range orders.

In conclusion, we report results of temperature-dependent neutron powder diffraction and spectroscopy experiments. Diffraction data collected between 300 and 0.5 K reveal no signature of a structural phase transition or of the predicted long-range magnetic orders. However, careful inspection of the low-temperature thermal expansion shows a subtle response of the c axis to the onset of superconductivity. Analyses of the internal bonding of the DWS reveal a similar response to T_c where the CrAs plaquettes become less noncentrosymmetric due to a strong contraction of the Cr2-Cr2 bond length. Neutron spectroscopy experiments show the presence of a column of scattering centered at a wave vector $q_m = 00\frac{1}{2}$ which is suppressed below T_c and exhibits a Q dependence consistent with a magnetic origin. We propose that this inelastic signal indicates that $K_2Cr_3As_3$ is near a magnetic instability with a tendency to order possibly in an UUDD state. Spin-wave simulations of this structure replicate our observed inelastic signal and generally agree with predictions for the Cr-Cr magnetic interactions. Comparison of the UUDD magnetic structure with the observed bonding behavior at T_c is suggestive of competition between short-range magnetic order and superconductivity, hinting at a situation similar to that of the FBS. Furthermore, the presence of incipient magnetic order with an AFM q_m lends support to spin-singlet models of superconductivity in these materials and suggests local fluctuations available for mediating electron pairing are AFM in nature.

The part of the research that was conducted at ORNL's High Flux Isotope Reactor and Spallation Neutron Source was sponsored by the Scientific User Facilities Division, Office of Basic Energy Sciences, US Department of Energy. The research is partly supported by the US Department of Energy(DOE), Office of Science, Basic Energy Sciences (BES), Materials Science and Engineering Division. The authors thank S. Chi for providing help during experimental collection and analysis. ORNL is managed by UT-Battelle, LLC under Contract No. DE-AC05-00OR22725 with the US Department of Energy. The US Government retains and the publisher, by accepting the article for publication, acknowledges that the US Government retains a nonexclusive, paid-up, irrevocable, worldwide license to publish or reproduce the published form of this manuscript, or allow others to do so, for US Government purposes.

The Department of Energy will provide public access to these results of federally sponsored research in accordance with the DOE Public Access Plan [54].

[1] D. Basov and A. Chubukov, Nat. Phys. **7**, 272 (2011).

[2] J.-K. Bao, J.-Y. Liu, C.-W. Ma, Z.-H. Meng, Z.-T. Tang, Y.-L. Sun, H.-F. Zhai, H. Jiang, H. Bai, C.-M. Feng, Z.-A. Xu, and G.-H. Cao, Phys. Rev. X **5**, 011013 (2015).

[3] H. Jiang, G. Cao, and C. Cao, Sci. Rep. **5**, 16054 (2015).

[4] Z.-T. Tang, J.-K. Bao, Z. Wang, H. Bai, H. Jiang, Y. Liu, H.-F. Zhai, C.-M. Feng, Z.-A. Xu, and G.-H. Cao, Sci. China Mater. **58**, 16 (2015).

[5] X. F. Wang, C. Roncaioli, C. Eckberg, H. Kim, J. Yong, Y. Nakajima, S. R. Saha, P. Y. Zavalij, and J. Paglione, Phys. Rev. B **92**, 020508(R) (2015).

[6] X.-X. Wu, C.-C. Le, J. Yuan, H. Fan, and J.-P. Hu, Chin. Phys. Lett. **32**, 057401 (2015).

[7] P. Alemany and E. Canadell, Inorg. Chem. **54**, 8029 (2015).

[8] J.-J. Miao, F.-C. Zhang, and Y. Zhou, Phys. Rev. B **94**, 205129 (2016).

[9] L.-D. Zhang, X. Wu, H. Fan, F. Yang, and J. Hu, Europhys. Lett. **113**, 37003 (2016).

[10] H. Zhong, X.-Y. Feng, H. Chen, and J. Dai, Phys. Rev. Lett. **115**, 227001 (2015).

[11] J.-K. Bao, L. Li, Z.-T. Tang, Y. Liu, Y.-K. Li, H. Bai, C.-M. Feng, Z.-A. Xu, and G.-H. Cao, Phys. Rev. B **91**, 180404(R) (2015).

[12] H. Z. Zhi, T. Imai, F. L. Ning, J.-K. Bao, and G.-H. Cao, Phys. Rev. Lett. **114**, 147004 (2015).

[13] D. T. Adroja, A. Bhattacharyya, M. Telling, Y. Feng, M. Smidman, B. Pan, J. Zhao, A. D. Hillier, F. L. Pratt, and A. M. Strydom, Phys. Rev. B **92**, 134505 (2015).
[14] F. F. Balakirev, T. Kong, M. Jaime, R. D. McDonald, C. H. Mielke, A. Gurevich, P. C. Canfield, and S. L. Bud'ko, Phys. Rev. B **91**, 220505(R) (2015).
[15] H. Zuo, J.-K. Bao, Y. Liu, J. Wang, Z. Jin, Z. Xia, L. Li, Z. Xu, J. Kang, Z. Zhu, and G.-H. Cao, Phys. Rev. B **95**, 014502 (2017).
[16] G. M. Pang, M. Smidman, W. B. Jiang, J. K. Bao, Z. F. Weng, Y. F. Wang, L. Jiao, J. L. Zhang, G. H. Cao, and H. Q. Yuan, Phys. Rev. B **91**, 220502 (2015).
[17] M. D. Watson, Y. Feng, C. W. Nicholson, C. Monney, J. M. Riley, H. Iwasawa, K. Refson, V. Sacksteder, D. T. Adroja, J. Zhao, and M. Hoesch, Phys. Rev. Lett. **118**, 097002 (2017).
[18] A. Subedi, Phys. Rev. B **92**, 174501 (2015).
[19] X.-X. Wu, F. Yang, S. Qin, H. Fan, and J. Hu, arXiv:1507.07451.
[20] See Supplemental Material at http://link.aps.org/supplemental/10.1103/PhysRevB.96.180506 for details pertaining to sample synthesis, Rietveld refinement methodology, group theory analysis and spin-wave modeling.
[21] J. Rodríguez-Carvajal, Physica B **192**, 55 (1993).
[22] B. H. Toby, Powder Diffr. **21**, 67 (2006).
[23] J. Larsen, B. M. Uranga, G. Stieper, S. L. Holm, C. Bernhard, T. Wolf, K. Lefmann, B. M. Andersen, and C. Niedermayer, Phys. Rev. B **91**, 024504 (2015).
[24] L. W. Finger, D. E. Cox, and A. P. Jephcoat, J. Appl. Crystallogr. **27**, 892 (1994).
[25] S. Avci, J. M. Allred, O. Chmaissem, D. Y. Chung, S. Rosenkranz, J. A. Schlueter, H. Claus, D. D. Khalyavin, P. Manuel, A. Llobet, M. R. Suchomel, M. G. Kanatzidis, and R. Osborn, Phys. Rev. B **88**, 094510 (2013).
[26] J. M. Allred, K. M. Taddei, D. E. Bugaris, S. Avci, D. Y. Chung, H. Claus, C. dela Cruz, M. G. Kanatzidis, S. Rosenkranz, R. Osborn, and O. Chmaissem, Phys. Rev. B **90**, 104513 (2014).
[27] K. M. Taddei, J. M. Allred, D. E. Bugaris, S. Lapidus, M. J. Krogstad, R. Stadel, H. Claus, D. Y. Chung, M. G. Kanatzidis, S. Rosenkranz, R. Osborn, and O. Chmaissem, Phys. Rev. B **93**, 134510 (2016).
[28] M. Potel, R. Chevrel, and M. Sergent, Acta Crystallogr., Sect. B **36**, 1545 (1980).
[29] R. Brusetti, A. J. Dianoux, P. Gougeon, M. Potel, E. Bonjour, and R. Calemczuk, Europhys. Lett. **10**, 563 (1989).
[30] Z.-T. Tang, J.-K. Bao, Y. Liu, Y.-L. Sun, A. Ablimit, H.-F. Zhai, H. Jiang, C.-M. Feng, Z.-A. Xu, and G.-H. Cao, Phys. Rev. B **91**, 020506 (2015).
[31] Z. Wang, W. Yi, Q. Wu, V. A. Sidorov, J. Bao, Z. Tang, J. Guo, Y. Zhou, S. Zhang, H. Li, Y. Shi, X. Wu, L. Zhang, K. Yang, A. Li, G. Cao, J. Hu, L. Sun, and Z. Zhao, Sci. Rep. **6**, 37878 (2016).
[32] M. Rotter, M. Pangerl, M. Tegel, and D. Johrendt, Angew. Chem., Int. Ed. **47**, 7949 (2008).
[33] F.-C. Hsu, J.-Y. Luo, K.-W. Yeh, T.-K. Chen, T.-W. Huang, P. M. Wu, Y.-C. Lee, Y.-L. Huang, Y.-Y. Chu, D.-C. Yan, and M.-K. Wu, Proc. Natl. Acad. Sci. USA **105**, 14262 (2008).
[34] K. M. Taddei, M. Sturza, D. Y. Chung, H. B. Cao, H. Claus, M. G. Kanatzidis, R. Osborn, S. Rosenkranz, and O. Chmaissem, Phys. Rev. B **92**, 094505 (2015).
[35] A. E. Böhmer, F. Hardy, F. Eilers, D. Ernst, P. Adelmann, P. Schweiss, T. Wolf, and C. Meingast, Phys. Rev. B **87**, 180505 (2013).
[36] R. Lortz, C. Meingast, D. Ernst, B. Renker, D. D. Lawrie, and J. P. Franck, J. Low Temp. Phys. **131**, 1101 (2003).
[37] M. Miyakawa, R. Y. Umetsu, K. Fukamichi, H. Yoshida, and E. Matsubara, J. Phys.: Condens. Matter **15**, 4817 (2003).
[38] M. Miyakawa, R. Y. Umetsu, M. Ohta, A. Fujita, K. Fukamichi, and T. Hori, Phys. Rev. B **72**, 054420 (2005).
[39] M. Miyakawa, R. Y. Umetsu, and K. Fukamichi, J. Phys.: Condens. Matter **13**, 3809 (2001).
[40] K. M. Taddei, J. M. Allred, D. E. Bugaris, S. H. Lapidus, M. J. Krogstad, H. Claus, D. Y. Chung, M. G. Kanatzidis, R. Osborn, S. Rosenkranz, and O. Chmaissem, Phys. Rev. B **95**, 064508 (2017).
[41] R. Osborn, E. A. Goremychkin, A. I. Kolesnikov, and D. G. Hinks, Phys. Rev. Lett. **87**, 017005 (2001).
[42] H. Zhi, D. Lee, T. Imai, Z. Tang, Y. Liu, and G. Cao, Phys. Rev. B **93**, 174508 (2016).
[43] J. Yang, Z. T. Tang, G. H. Cao, and G.-q. Zheng, Phys. Rev. Lett. **115**, 147002 (2015).
[44] M. C. Rahn, R. A. Ewings, S. J. Sedlmaier, S. J. Clarke, and A. T. Boothroyd, Phys. Rev. B **91**, 180501 (2015).
[45] A. E. Taylor, M. J. Pitcher, R. A. Ewings, T. G. Perring, S. J. Clarke, and A. T. Boothroyd, Phys. Rev. B **83**, 220514 (2011).
[46] B. J. Campbell, H. T. Stokes, D. E. Tanner, and D. M. Hatch, J. Appl. Crystallogr. **39**, 607 (2006).
[47] S. Toth and B. Lake, J. Phys.: Condens. Matter **27**, 166002 (2015).
[48] C. Cao, H. Jiang, X.-Y. Feng, and J. Dai, Phys. Rev. B **92**, 235107 (2015).
[49] B. A. Frandsen, K. M. Taddei, M. Yi, A. Frano, Z. Guguchia, R. Yu, Q. Si, D. E. Bugaris, R. Stadel, R. Osborn, S. Rosenkranz, O. Chmaissem, and R. J. Birgeneau, Phys. Rev. Lett. **119**, 187001 (2017).
[50] R. M. Fernandes, A. E. Böhmer, C. Meingast, and J. Schmalian, Phys. Rev. Lett. **111**, 137001 (2013).
[51] S. Nandi, M. G. Kim, A. Kreyssig, R. M. Fernandes, D. K. Pratt, A. Thaler, N. Ni, S. L. Bud'ko, P. C. Canfield, J. Schmalian, R. J. McQueeney, and A. I. Goldman, Phys. Rev. Lett. **104**, 057006 (2010).
[52] J. M. Allred, K. M. Taddei, D. E. Bugaris, M. J. Krogstad, S. H. Lapidus, D. Y. Chung, H. Claus, M. G. Kanatzidis, D. E. Brown, J. Kang, R. M. Fernandes, I. Eremin, S. Rosenkranz, O. Chmaissem, and R. Osborn, Nat. Phys. **12**, 493 (2016).
[53] W.-L. Zhang, H. Li, D. Xia, H. W. Liu, Y.-G. Shi, J. L. Luo, J. Hu, P. Richard, and H. Ding, Phys. Rev. B **92**, 060502 (2015).
[54] http://energy.gov/downloads/doe-public-access-plan.